Molecular Biology of the Cell
Vol. 15, 1690–1701, April 2004

Syntaxin-6 SNARE Involvement in Secretory and Endocytic Pathways of Cultured Pancreatic β-Cells

Regina Kuliawat,* Elena Kalinina,† Jason Bock,‡ Lloyd Fricker,† Timothy E. McGraw,§ Se Ryoung Kim,* Jiayu Zhong,* Richard Scheller,‖ and Peter Arvan¶#

*Division of Endocrinology and Department of Developmental/Molecular Biology and †Department of Molecular Pharmacology, Albert Einstein College of Medicine, Bronx, New York 10461; ‡Human Genome Sciences, Inc., Rockville, Maryland 20850; §Department of Biochemistry and Structural Biology, Weill Medical College of Cornell University, New York, New York 10021; ‖Genentech, Inc., South San Francisco, California 94080; and ¶Division of Metabolism, Endocrinology, and Diabetes, University of Michigan Medical Center, Ann Arbor, Michigan 48109

Submitted August 4, 2003; Revised December 1, 2003; Accepted January 6, 2004
Monitoring Editor: Benjamin Glick

In pancreatic β-cells, the syntaxin 6 (Syn6) soluble *N*-ethylmaleimide-sensitive factor attachment protein receptor is distributed in the *trans*-Golgi network (TGN) (with spillover into immature secretory granules) and endosomes. A possible Syn6 requirement has been suggested in secretory granule biogenesis, but the role of Syn6 in live regulated secretory cells remains unexplored. We have created an ecdysone-inducible gene expression system in the INS-1 β-cell line and find that induced expression of a membrane-anchorless, cytosolic Syn6 (called Syn6t), but not full-length Syn6, causes a prominent defect in endosomal delivery to lysosomes, and the TGN, in these cells. The defect occurs downstream of the endosomal branchpoint involved in transferrin recycling, and upstream of the steady-state distribution of mannose 6-phosphate receptors. By contrast, neither acquisition of stimulus competence nor the ultimate size of β-granules is affected. Biosynthetic effects of dominant-interfering Syn6 seem limited to slowed intragranular processing to insulin (achieving normal levels within 2 h) and minor perturbation of sorting of newly synthesized lysosomal proenzymes. We conclude that expression of the Syn6t mutant slows a rate-limiting step in endosomal maturation but provides only modest and potentially indirect interference with regulated and constitutive secretory pathways, and in TGN sorting of lysosomal enzymes.

INTRODUCTION

The final membrane remodeling required for biogenesis of mature endocrine secretory granules occurs at the stage of clathrin-decorated, immature secretory granules (ISGs), in which a subset of lumenal proteins (Kuliawat *et al.*, 1997) and a subset of membrane proteins (Dittié *et al.*, 1997) are removed and delivered to the endosomal system (Feng and Arvan, 2003). Of the membrane proteins that are removed from ISGs, some play clear physiological roles in secretory granule biology (Milgram *et al.*, 1994); others may be involved in completion of *trans*-Gogi network (TGN)-based remodeling tasks (Klumperman *et al.*, 1998), whereas still others may have important or even primary functions in the endosomal system (Molloy *et al.*, 1999). In this report, we consider syntaxin 6 (Syn6), a soluble *N*-ethylmaleimide-sensitive factor attachment protein receptor (SNARE) protein found in ISG membranes (Klumperman *et al.*, 1998) as well as TGN and endosome compartments (Bock *et al.*, 1997; Mallard *et al.*, 2002). Despite a common assembly scheme, SNARE protein interactions are now generally recognized to provide an important part of the specificity of intracellular membrane fusion events (Parlati *et al.*, 2000; Scales *et al.*, 2000; Bock *et al.*, 2001; Parlati *et al.*, 2002) as well as part of the driving force for membrane fusion (Hu *et al.*, 2003). In the four-helix bundle contributing to a functional SNARE complex, Syn6 acts as a "light chain" (Fukuda *et al.*, 2000) homologous to the C-terminal helix of SNAP-25 (Bock *et al.*, 2001; Misura *et al.*, 2002). In some cases Syn6 has been found by coimmunoprecipitation to be present in SNARE complexes that include Syn7, Vti1b, and vesicle-associated membrane protein (VAMP)7 or VAMP8, as part of fusion events within endosomal system (Wade *et al.*, 2001).

Some SNARE proteins may be present in ISGs as a prelude to their role in stimulus-dependent granule exocytosis (Regazzi *et al.*, 1996; Wheeler *et al.*, 1996). However at steady state, molecules such as VAMP4 and Syn6 are distributed in the TGN and ISGs but not in mature secretory granules (Bock *et al.*, 1997; Klumperman *et al.*, 1998; Steegmaier *et al.*, 1999; Eaton *et al.*, 2000; Hinners *et al.*, 2003). Furthermore, VAMP4 and Syn6 are also found abundantly in the endosomes, suggesting recycling of these SNARE proteins between biosynthetic and endocytic pathways (Wendler and Tooze, 2001). It is unclear whether these proteins play roles in membrane fusion events at all stages of their intracellular transport itinerary (Watson and Pessin, 2000). Clearly, steady-state localization does not necessarily establish where the primary intracellular activity of that protein occurs. A case in point is the cation-independent mannose

Article published online ahead of print. Mol. Biol. Cell 10.1091/mbc.E03–08–0554. Article and publication date are available at www.molbiolcell.org/cgi/doi/10.1091/mbc.E03–08–0554.

Corresponding author. E-mail address: parvan@umich.edu.

6-phosphate receptor: there is a major steady-state distribution of the receptor in endosomes (Griffiths *et al.*, 1988), even though initial capture of newly synthesized lysosomal enzymes by the receptor occurs in the TGN.

To date, ISGs have been reported to be associated with three different kinds of membrane fission/fusion events that may involve SNAREs: direct exocytosis of clathrin-decorated ISGs at the cell surface (Orci *et al.*, 1984; Molinete *et al.*, 2001); clathrin-coated vesicle budding that initiates the constitutive-like secretory pathway and facilitates delivery of lysosomal proenzymes to the endosomal system (Kuliawat and Arvan, 1992; Kuliawat and Arvan, 1994); and homotypic ISG-ISG fusion, which might be an obligatory step in mature secretory granule biogenesis (Tooze *et al.*, 1991; Urbe *et al.*, 1998). It is not clear which, if any, of these fission/fusion events in living cells use Syn6 in a rate-limiting step. To explore such rate-limiting steps, we have been interested to perturb intracellular Syn6 function in the pancreatic β-cell line INS-1. We have not pursued microinjection of blocking antibodies because of an interest to generate biochemical as well as morphological phenotypes, and because preliminary investigations have indicated that INS-1 cells are more difficult to microinject than non-β-cell lines. Alternatively, soluble SNARE protein mutants lacking integral membrane anchors are competent to form complexes with endogenous SNAREs and ancillary proteins and have been repeatedly found to cause specific dominant interference of membrane fusion events facilitated by their endogenous counterparts (Dascher and Balch, 1996; Olson *et al.*, 1997; Scales *et al.*, 2000; Hua and Scheller, 2001; Collins *et al.*, 2002; Geelen *et al.*, 2002; Xu *et al.*, 2002; Li *et al.*, 2003; Low *et al.*, 2003). Therefore, with this strategy in mind, we have developed an inducible gene expression system in the INS-1 pancreatic β-cell line and used this system to carefully analyze a series of phenotypes associated with induced expression of full-length Syn6 or a truncated, membrane-anchorless form, Syn6t. Our results suggest specific Syn6 involvement in endosomal function in pancreatic β-cells.

MATERIALS AND METHODS

Antibodies and Other Materials

A rabbit polyclonal antibody against retinoid X receptor$_\alpha$ was from Santa Cruz Biotechnology (sc553; Santa Cruz Biotechnology, Sant Cruz, CA). The monoclonal antibody (mAb) 3D10 against the N-terminal 26 residues of the Syn6 cytosolic domain has been described previously (Bock *et al.*, 1997) and was used for Western blotting and immunoprecipitation. A mAb against Syn6 used for immunofluorescence was from StressGen Biotechnologies (San Diego, CA). Both polyclonal and monoclonal antibodies against the c-myc epitope were from Santa Cruz Biotechnology. Guinea pig anti-insulin was from Linco Research (St. Charles, MO). Rabbit polyclonal anti-procathepsin B was from Upstate Biotechnology (Lake Placid, NY). Rabbit polyclonal anti-TGN38 was the kind gift of Dr. S. Milgram (University of North Carolina, Chapel Hill, NC). A mouse ascites containing mAb clone 2F7.1 against rat TGN38 (Luzio *et al.*, 1990) was from Affinity Bioreagents (Golden, CO). Two mAbs against Tac were from American Type Culture Collection (clones 2A3A1H and 7G7B6), with similar results. Rabbit polyclonal antiserum specific for Vti1b was generously provided by the lab of Dr. J. E. Rothman (Memorial Sloan-Kettering Cancer Center, New York, NY). Rabbit polyclonal anti-Vti1a and mouse monoclonal anti-EEA1 were from BD Transduction Laboratories (Lexington, KY). Rabbit polyclonal anti-Ykt6 was from Dr. J. Hay (University of Michigan, Ann Arbor, MI). A mouse mAb (E2-1) directed against SFV-E2 (Kielian *et al.*, 1990) was the kind gift of Dr. M. Kielian (Albert Einstein College of Medicine, Bronx, NY). A rabbit polyclonal antiserum against rat brain carboxypeptidase D (CPD) was described previously (Varlamov and Fricker, 1998). All antibodies used in live cell uptake experiments were azide free. Anti-calnexin was from Dr. P. Kim (University of Cincinnati College of Medicine, Cincinnati, OH), anti-synaptophysin/p38 was obtained from the laboratory of Dr. D. Shields (Albert Einstein College of Medicine), and anti-guanine nucleotide dissociation inhibitor (GDI) was from Zymed Laboratories (South San Francisco, CA). Horseradish peroxidase-, fluorescein isothiocyanate-, and Cy3- and Cy2-conjugated secondary antibodies were from Jackson ImmunoResearch Laboratories (West Grove, PA). [^{35}S]Methionine/cysteine (Expre^{35}S^{35}S) was from PerkinElmer Life Sciences (Boston, MA). Methionine/cysteine-deficient and complete DME, RPMI 1640 medium, leupeptin, pepstatin, and stock chemicals were from Sigma-Aldrich (St. Louis, MO).

Cell Culture

INS-1 cells were cultured in RPMI 1640 medium supplemented with 30 mM sodium bicarbonate, 1 mM sodium pyruvate, 10 mM HEPES, pH 7.35, 50 μM β-mercaptoethanol, 10% fetal bovine serum, and 0.1% penicillin-streptomycin (Invitrogen, Carlsbad, CA) at 37°C with 5% CO_2 as described previously (Neerman-Arbez and Halban, 1993).

DNA Constructs

An N-terminally myc-tagged full-length Syn6 was prepared by polymerase chain reaction mutagenesis with flanking 5′ *Cla*I and 3′ *Hin*dIII sites; this was subcloned into these sites in pCMV4. In addition, Syn6t was prepared by polymerase chain reaction mutagenesis with flanking 5′ *Bgl*II and a 3′ sequence encoding a myc tag and a *Hin*dIII site, and this was also subcloned into pCMV4. (Recent studies indicate that both N-terminally tagged an C-terminally tagged syntaxins exhibit normal intracellular trafficking and distribution; Kasai and Akagawa, 2001.) Both full-length and Syn6t inserts were excised from pCMV4 with *Bgl*II/*Xba*I and subcloned into pIND (Invitrogen). The plasmids encoding Tac-TGN38 (Humphrey *et al.*, 1993; Ghosh *et al.*, 1998) and Tac-Lamp1 (Marks *et al.*, 1996) chimeras were kindly provided by Dr. M.S. Marks (University of Pennsylvania School of Medicine, Philadelphia, PA). The albumin-CPD chimera has been previously described (Kalinina and Fricker, 2003).

Transfection

Transfection of plasmid DNA was with Effectine (QIAGEN, Valencia, CA) following the manufacturer's protocol. Stable INS-1 clones transfected with pVgRXR (Invitrogen) were selected with 40 μg/ml zeocin; INS cells positively expressing both ecdysone receptor and retinoid X receptor$_\alpha$ by Western blot were termed INS39 cells. INS39 cells were then transfected with the pIND vector to achieve inducible expression of full-length or truncated forms of myc-tagged Syn6, and clones were selected in 20 μg/ml zeocin plus 100 μg/ml G418 (Invitrogen) and maintained in the presence of 20 μg/ml zeocin, 50 μg/ml G418. All antibiotics were removed at least 2 d before the beginning of experiments. For transient expression experiments, cells were used 2 d after transfection.

Uptake and Degradation of ^{35}S-Semliki Forest Virus (SFV)

[^{35}S]Methionine-labeled Semliki Forest virus was the kind gift of Dr. Margaret Kielian (Albert Einstein College of Medicine). INS cells grown in 35-mm plates were either uninduced or induced by the addition of 20 μM ponasterone (Invitrogen) for 24 h before experiments. The cells were then incubated for 1.5 h at 4°C with [^{35}S]methionine-labeled Semliki Forest virus. After several washes in cold medium to remove unbound virus, internalization and degradation of surface-bound SFV were determined as described previously (Kielian *et al.*, 1990).

Transferrin Recycling Assay

Cells were grown on 24-well plates; all experimental observations were made in triplicate. To achieve steady state, cells were incubated with 3 μg/ml ^{125}I-transferrin in McCoy's binding buffer for 90 min at 37°C (a 200-fold excess of unlabeled transferrin was added to some wells to determine nonspecific binding). Before starting the assay, cells were acid washed for 2 min in 0.15 M NaCl, 20 mM citrate, pH 5.0, to remove surface-bound ^{125}I-transferrin, followed by washing in 150 mM NaCl, 1 mM $CaCl_2$, 5 mM KCl, 1 mM $MgCl_2$, and 20 mM HEPES, pH 7.4. The cells were then incubated in the presence of 3 μg/ml unlabeled transferrin and 10 mM desferroxamine at 37°C. At 2.5, 5, 10, 15, and 20 min, the medium was collected to measure ^{125}I-transferrin efflux, the cells were solubilized, and radioactivity in both was measured by scintillation counting.

Metabolic Labeling and Stimulation of Secretory Granule Exocytosis

Stably transfected INS-1 clones were seeded 2 d before experiments in the absence of selectable antibiotics. Cells were induced by the addition of 20 μM ponasterone for 24 h before experiments. Cells were preincubated for 30 min in methionine and cysteine-free DME and then pulse labeled with 130 μCi of [^{35}S]methionine/cysteine for 30 min in the same medium. After labeling, cells were washed three times with ice-cold DME before chase for various times at 37°C in DME containing 5.5 mM glucose and 1% fetal bovine serum. Exocytosis was stimulated in DME containing a combination secretagogue, including 10 mM glucose, 1 μM phorbol 12-myristate 13-acetate, 1 mM isobutylmethylxanthine, 1 mM tolbutamide, 10 mM leucine, and 10 mM glutamine (Neerman-Arbez and Halban, 1993). At the end of selected chase periods, media were collected, and cells were lysed in 1% Triton X-100, 0.1% SDS, 100

mM NaCl, 10 mM EDTA, 25 mM Tris, pH 7.4, plus 1 mU/ml aprotinin, 1 μM leupeptin, 10 μM pepstatin, 5 mM EDTA, 1 μM E64, and 1 mM iodoacetamide. Cell lysates and chase media were precleared with zysorbin (Zymed Laboratories), normalized to 200,000 trichloroacetic acid precipitable cpm, and subjected to immunoprecipitation.

Western Blotting of Syn6

Western Blotting of Syn6 was performed on samples subjected to 10% SDS-PAGE, electrotransferred to nitrocellulose, and blotted with primary antibody against c-myc or syntaxin 6 at 1:1000 dilution and the appropriate secondary IgG-peroxidase conjugate at 1:2000 dilution, followed by enhanced chemiluminescence detection.

Cell Surface Tagging and Recycling of CPD, Albumin-CPD, and Tac-TGN38 to the TGN

Cells grown on poly-L-lysine–coated coverslips were treated plus or minus 20 μM ponasterone for 24 h. For antibody uptake, cells were incubated either with rabbit anti-albumin (1:150 dilution) or mouse mAb anti-Tac. At the conclusion of the uptake period, the cells were washed twice in ice-cold phosphate-buffered saline (PBS) and fixed with 4% formaldehyde for 15 min, washed, permeabilized with 0.1% Triton X-100 in PBS for 15 min, and stained with Cy3-conjugated IgG secondary antibody at 1:500 dilution. In addition, these fixed permeabilized cells were incubated with anti-TGN38 (either rabbit polyclonal or mouse mAb, depending upon which antibody was used for uptake) and a Cy2-conjugated anti-mouse IgG secondary antibody at 1:100 dilution.

Electron Microscopy

Syn6-21 cells and Syn6t-10 cells plus and minus 1 d of ponasterone treatment, grown on tissue culture plastic, were fixed with 2.5% glutaraldehyde and 2% formaldehyde in 0.1 M Na cacodylate, pH 7.0, for 2 h at room temperature and postfixed with 1% osmium tetroxide. The cells were dehydrated in ethanol and propylene oxide, infiltrated and embedded in LX112 resin (LADD Research Industries, Burlington, VT), thin sectioned, stained with lead citrate and 1% uranyl acetate, and examined at a fixed magnification in a 1200EX transmission electron microscope (JEOL, Tokyo, Japan) at 80 kV. Captured images were then projected and each individual secretory granule profile outlined and analyzed for precise granule cross-sectional area by the Investigator HT Analyzer program (version 2.1; Genomic Solutions, Ann Arbor, MI). Finally, mean granule diameters were calculated from the cross-sectional areas, based on a spherical geometry.

Membrane Sedimentation and Sucrose-Velocity Gradient Centrifugation Assays

Cells grown on 15-cm dishes were either uninduced or induced for 24 h with 20 μM ponasterone. The cells were washed twice with ice-cold PBS plus 0.2 mM $MgCl_2$, plus 1 mU/ml aprotinin, 1 μM leupeptin, 10 μM pepstatin, 5 mM EDTA, 1 μM E64, and 1 mM iodoacetamide. For membrane sedimentation, the cells were scraped and lysed in buffered 0.3 M sucrose plus protease inhibitors by eight passages through 21-gauge needle followed by eight passages through a ball-bearing cell cracker with 0.002-inch clearance. Then, 0.5 ml of cell homogenate was spun at 67,500 $\times$ *g*·h. Pellets were resuspended in an equal volume of the same buffer, and equal aliquots of pellet and supernatant fractions were taken for SDS-PAGE and immunoblotting. In preparation for sucrose-velocity gradient centrifugation, cells were lysed the same way but in 0.1 M KCl, 1 mM EDTA, 1% glycerol, and 10 mM HEPES, pH 7.35, plus protease inhibitors. Postnuclear supernatants were loaded onto 5–20% HEPES-buffered sucrose gradients, spun in swinging buckets for 1 h at 100,000 $\times$ *g*, and collected in 12 fractions, with fraction 12 including the resuspended pellet. The fractions were analyzed by SDS-PAGE and immunoblotting.

RESULTS

Inducible Expression of Syn6 and Syn6t in INS Cells

Because soluble cytosolic domains of a variety of syntaxins have been found to confer dominant interfering phenotypes (Dascher and Balch, 1996; Olson *et al*., 1997; Scales *et al*., 2000; Hua and Scheller, 2001; Collins *et al*., 2002; Geelen *et al*., 2002; Xu *et al*., 2002; Low *et al*., 2003; Li *et al*., 2003), we wished to create inducible expression of a dominant interfering, membrane-anchorless form of Syn6 in a pancreatic β-cell line. For this purpose, ecdysone receptor/retinoid X receptor$_\alpha$-expressing INS cells (called INS39) were transfected with a vector driving the ponasterone-inducible expression of a myc-tagged Syn6$_{1\rightarrow236}$, called Syn6t. Two Syn6t-expressing clones (6t-1 and 6t-10) were studied; uninduced cells exhibited no mutant phenotypes, whereas induction of Syn6t expression in both clones exhibited identical mutant phenotypes (see below). To simplify, many of the experiments presented herein show results of Syn6t expression in only one of the clones. Untransfected INS39 cells, parental INS-1 cells, or INS39 cells inducibly expressing a myc-tagged full-length Syn6 (usually clone Syn6-21) were used as control cell lines in various experiments.

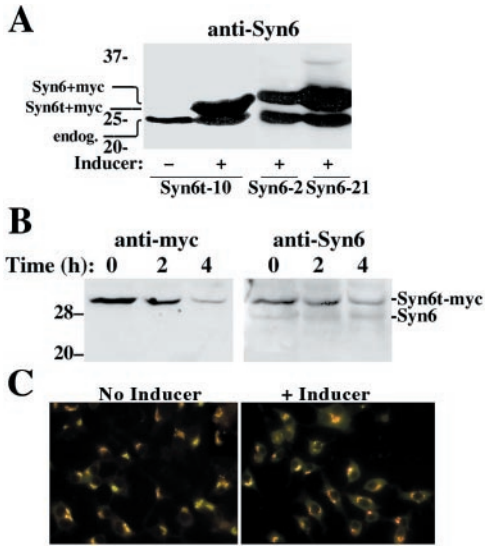

Figure 1. Expression of full-length Syn6 and a truncated membrane-anchorless form (Syn6t), tagged with a c-myc epitope. (A) Western blotting with mAb 3D10 (against Syn6 cytosolic domain) of Syn6t-10, Syn6-2, or Syn6-21 cells either uninduced (−) or induced by the addition of 20 μM ponasterone (+) 24 h before cell lysis. (B) Western blot with a polyclonal anti-myc antibody in ponasterone induced Syn6t-10 cells incubated for the indicated times in 10 μg/ml cycloheximide to inhibit new protein synthesis; the identical samples were also probed with mAb 3D10 against Syn6. Note the presence of endogenous ("endog.") Syn6 in A and B. (C) Immunofluorescence localization of endogenous TGN38 (primary mouse mAb, stained in green) and CPD (primary rabbit polyclonal antibody, stained in red) in Syn6t-10 cells in the absence and presence of inducer. An identical steady-state distribution was also observed upon induced expression of full-length Syn6 (our unpublished data).

After overnight induction of gene expression in the presence of ponasterone, immunoblotting with a monoclonal anti-Syn6 revealed inducible expression of Syn6t (~29 kDa) in the Syn6t-10 clone or full-length Syn6 (~30 kDa) in Syn6-2 and Syn6-21 clones, respectively (Figure 1A). In addition, all INS cells express the ~26-kDa endogenous Syn6 (Figure 1A). After 24 h of ponasterone treatment, the 6t-10 clone showed levels of Syn6t ~5.5-fold (n = 6) greater than endogenous Syn6 and Syn6-21 showed levels of full-length Syn6 ~4.4-fold greater (n = 8) than endogenous Syn6. Not surprisingly, Syn6t had a shorter half-life than endogenous Syn6, which showed no decrease in levels of immunoreactive protein in cells 4 h after cycloheximide treatment (Figure 1B). Immunofluorescence with anti-myc indicated that ≥90% of INS cells are positive for induced Syn6t expression; nevertheless in the cell population with induced expression of truncated (or full-length) Syn6, the steady-state juxtanuclear distributions of endogenous CPD and TGN38, two TGN markers, did not seem altered (Figure 1C). As shown in Figure 2A, whereas full-length myc-tagged Syn6 behaved as expected for an integral membrane protein (being quantita-

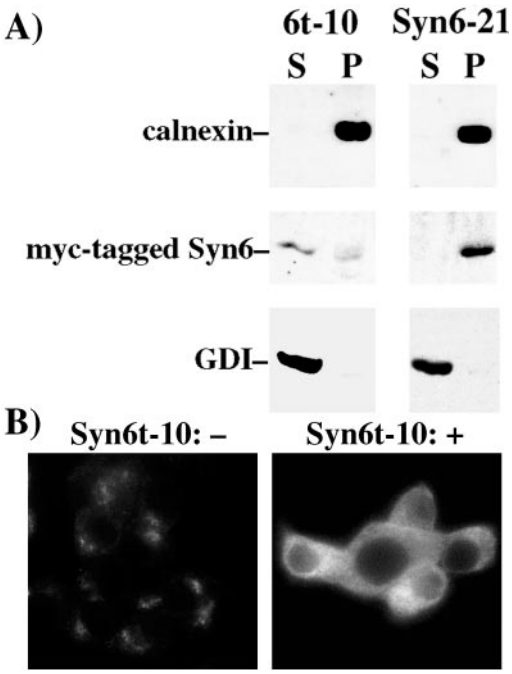

Figure 2. Extent of membrane association of inducibly expressed full-length Syn6 in Syn6-21 cells, and Syn6t in 6t-10 cells. (A) Homogenates were resolved into supernatant (S) and pellet (P) fractions as described in MATERIALS AND METHODS and analyzed by SDS-PAGE and Western blotting with antibodies against calnexin, myc tag, or GDI as indicated. (B) Immunofluorescence with anti-Syn6 mAb in uninduced (−) or induced (+) Syn6t-10 cells.

tively sedimented at 100,000 × *g* for 1 h, comparable with the control membrane protein, calnexin), myc-tagged Syn6t distributed primarily as a soluble protein with most occurring in the 100,000 × *g* supernatant (marked by the guanine nucleotide dissociation inhibitor [GDI] control protein). This difference was also apparent at the immunofluorescence level; although in the absence of inducer the endogenous Syn6 expressed in Syn6t-10 cells showed a juxtanuclear distribution (Figure 2B, left), after treatment with inducer the overall immunofluorescence of Syn6 was increased and weighted toward a diffuse cytosolic distribution (Figure 2B, right).

Dominant Negative Syn6t Causes Specific Defects in the Endosomal System of INS Cells

To evaluate endosomal function, we first examined whether Syn6t affected the lysosomal delivery/degradation of ligands endocytosed via the well-established clathrin-coated vesicle pathway. For this, we used a standard assay measuring lysosomal degradation of endocytosed ^{35}S-labeled SFV (Martys *et al.*, 1996) that has been previously examined in pancreatic β-cells (Turner and Arvan, 2000). Lysosomal delivery/degradation of ^{35}S-labeled SFV was statistically indistinguishable between INS cells, INS39 cells, INS39 cells transfected with full-length Syn6 in the absence or presence of inducer, or Syn6t-10 cells in which Syn6t was not expressed. However, after induction of Syn6t expression, there was dramatic inhibition of the rate of SFV degradation (Figure 3A). The magnitude of this effect is large; greater than or equal to the inhibition obtained upon 100 nM wortmannin addition to Chinese hamster ovary cells (Martys *et al.*, 1996) or 10 μg/ml brefeldin A added to INS-1 pancreatic β-cells (Turner and Arvan, 2000). Because no significant differences in surface binding or initial internalization of surface-bound SFV were observed (SFV uptake at 5 min is shown visually in Figure 5; see below), the data suggest that Syn6t induces a dominant interfering phenotype during endosome–lysosome maturation in INS cells.

To test whether the endosomal defect induced by Syn6t was in the most proximal portion of the endocytic pathway, we examined transferrin uptake and recycling from these cells. Not only was Syn6t expression without effect on transferrin uptake (our unpublished data), it also had no effect on transferrin return from the endocytic pathway, via recycling endosomes, back to the medium (Figure 3B). This suggests that the endosomal defect induced by Syn6t is located downstream of the transferrin recycling branchpoint.

To determine whether a similar endocytic pathway defect could be identified for another marker that defines the endosome–lysosome trafficking route, we transiently transfected INS cells to express a Tac-Lamp1 chimeric protein (Marks *et al.*, 1996) in which the cytoplasmic tail of Lamp1 was appended to the lumenal and transmembrane domains of a monomeric integral membrane reporter protein, the interleukin-2 receptor alpha-chain (Tac). In either INS39 cells or Syn6-21 cells after 1 h continuous uptake at 37°C, anti-Tac lumenal domain mAb had not yet reached cathepsin B-positive lysosomes in most cells (only 25% of cells showing complete colocalization), but at 2 h uptake, anti-Tac colocalized with cathepsin B-positive lysosomes (Figure 4,

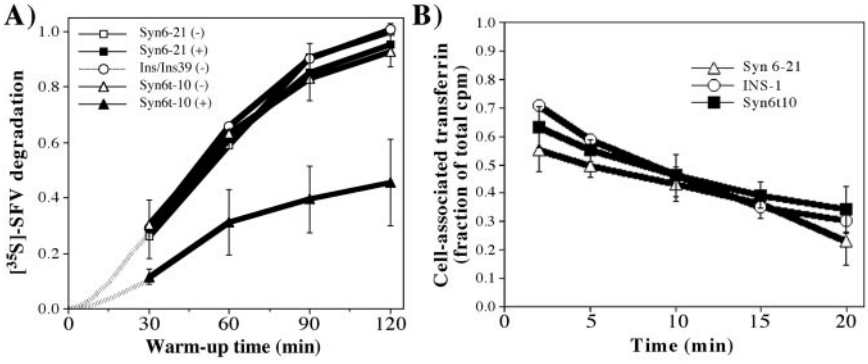

Figure 3. Endocytic pathway phenotype associated with dominant-interfering Syn6t expression. (A) Lysosomal delivery/degradation of [^{35}S]SFV is inhibited by induced expression of Syn6t. The assay was performed as described in MATERIALS AND METHODS. After 2 h of warm up, the fraction of total radioactivity bound to uninduced Syn6-21 cells that became degraded and occurred as trichloroacetic acid-soluble counts in the medium was ~35%; this was arbitrarily assigned a value of 1.0 and all other cells, conditions, and time points were compared with this value. The hatched lines indicate curves extrapolated to zero. (B) Recycling of ligand-bound transferrin receptors. After the cells indicated were loaded to steady state with ^{125}I-transferrin, the cells were washed and recycling of transferrin receptors to the cell surface was followed by release of ^{25}I-transferrin into the medium (and disappearance from cells).

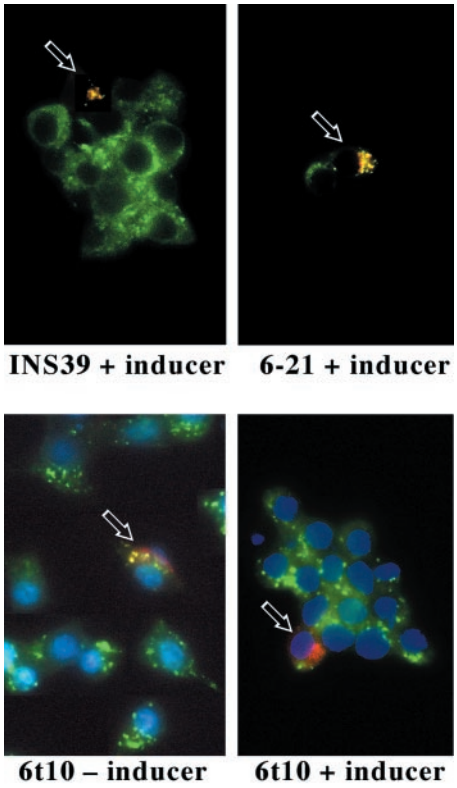

Figure 4. Continuous uptake of anti-Tac mAb in various INS cell clones transiently transfected to express a Tac-Lamp1 chimera. Transfected cells are indicated with arrows. Immunofluorescence distribution of cathepsin B-positive lysosomes is shown in green. The 2-h uptake of anti-Tac is detected by a Cy3-conjugated secondary antibody, shown in red. Regardless of the presence or absence of ponasterone, in cells not expressing Syn6t the Tac-Lamp1 chimera reaches cathepsin B-positive compartments. Note that in cells expressing Syn6t, the Tac-Lamp1 chimera shows delayed delivery to cathepsin B-positive compartments (bottom right).

top, marked with arrows) in most transfected cells. Specifically, when scored more than six experiments for cells that did not express Syn6t, all cells expressing Tac-Lamp1 showed either complete (50%) or partial (50%) colocalization of anti-Tac with cathepsin B-positive lysosomes, and this was also true in Syn6t-10 cells that were not treated with inducer (Figure 4, bottom left). However, in the majority (55%) of Syn6t-10 cells treated with inducer, the Tac-Lamp1 chimera had not yet achieved any delivery to lysosomes at 2 h (Figure 4, bottom right), whereas another 36% of cells showed only partial delivery.

It is easier to perform morphological studies of the endocytic pathway by using SFV rather than the Tac-Lamp1 chimera because the former method does not require transfection, and endocytosis of the antigenic marker occurs in >95% of cells. A mAb against the E2 epitope was used to track SFV after it had been prebound to the cell surface at 4°C (Figure 5A). Five minutes after warm up of cells to 37°C, virus was detected at the cell perimeter (Figure 5A, top). In whole cell immunofluorescence using cells with induced expression of full-length Syn6, by 20 min after warm up, virions could clearly be chased into the cell interior; but beginning after 35 min, the epitope to which the anti-E2 mAb was directed became substantially less immunoreactive (Figure 5A, bottom left), suggesting epitope masking, a conformational change, or degradation. By contrast, in cells with induced Syn6t expression, the intracellular staining intensity of the SFV E2 epitope largely persisted (Figure 5A, bottom right). To determine whether, at this time, virions had advanced as far as mannose-phosphate receptor-positive late endosomes, the experiment was repeated but this time by using confocal immunofluorescence microscopy and double labeling with anti-E2 and anti-mannose-phosphate receptor antibodies (Figure 5B). Once again in both types of INS cells the SFV particles initially decorated the cell perimeter and by 35 min after warm up, cells with induced expression of the full-length protein exhibited a significant decrease in detection of the E2 epitope (Figure 5B, bottom left). At this time in cells with induced expression of Syn6t (Figure 5B, bottom right), SFV immunofluorescence persisted (red), but the staining did not significantly colocalize with mannose-phosphate receptors (green). Eventually, at later times, SFV immunofluorescence also disappeared in Syn6t-expressing cells (our unpublished data). These data strongly suggest that Syn6t induces a defect in delivery of SFV to later endosomal compartments where loss of immunofluorescence is likely to occur, although this is a kinetic block rather than a permanent one.

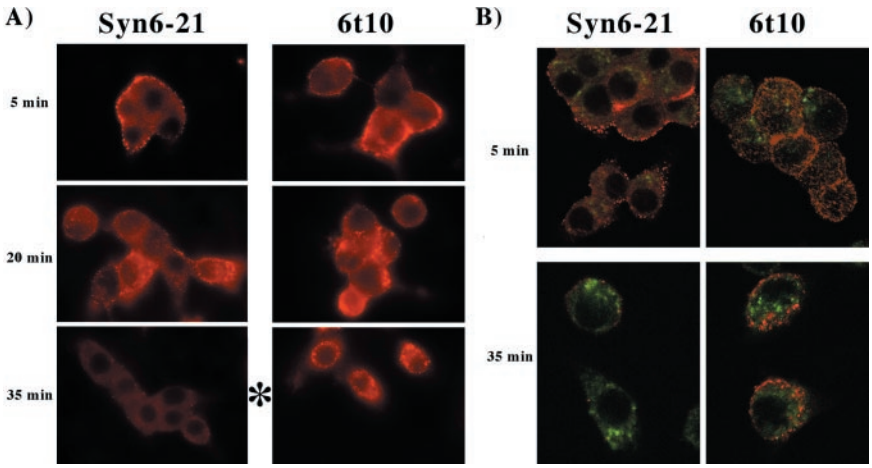

Figure 5. Progression of SFV through the endocytic pathway of INS cells. (A) Virus was prebound to the clones indicated at 4°C and the cells then washed thoroughly before warm up. At different times after warm up to 37°C, the cells were fixed, permeabilized, and immunostained using a mAb for the SFV E2 protein and a Cy3-conjugated secondary antibody (in red), and whole cell immunofluorescence captured with a charge-coupled device camera. (B) Samples were prepared as in A, but double labeled for SFV E2 (in red) and cation-independent mannose-phosphate receptors and a Cy2-conjugated secondary antibody (in green). The images were captured by confocal fluorescence.

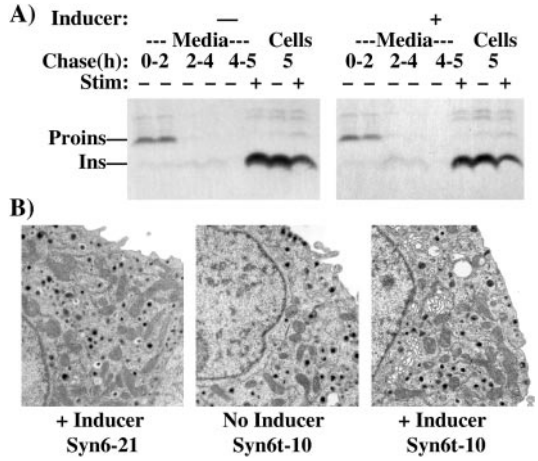

Figure 6. Biosynthesis of mature insulin secretory granules is not detectably affected by induced expression of Syn6t. (A) Syn 6t-10 cells either uninduced (−) or induced for 24 h with ponasterone (+) were pulse labeled, chased, and stimulated with secretagogue as described in the text. Proinsulin (Proins) and insulin (Ins) were recovered by immunoprecipitation with an anti-insulin antibody followed by SDS-PAGE and fluorography. (B) The cells as described below each panel were processed for electron microscopy as described in MATERIALS AND METHODS. A portion of the nucleus of the cell is oriented to the left of each image. The cells show relatively abundant secretory granules and mitochondria.

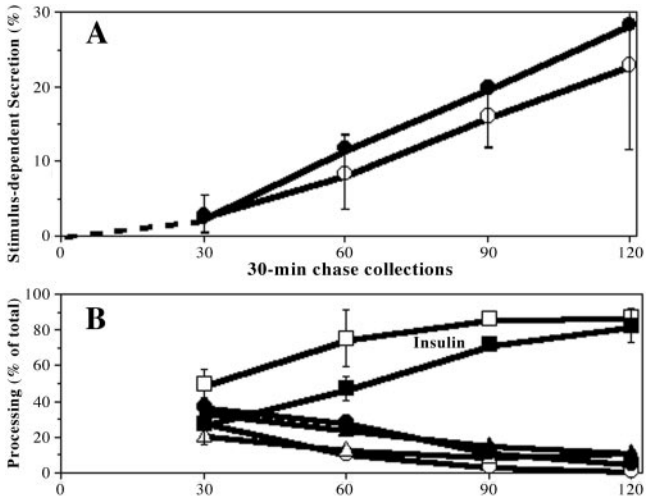

Figure 7. Biogenesis of new insulin secretory granules in cells expressing full-length Syn6 or Syn6t. Multiple wells of Syn 6-21 cells (open symbols) or 6t-10 cells (closed symbols) were induced for 24 h with ponasterone pulse labeled for 30 min and then chased for 30-min blocks of time: 0–30, 30–60, 60–90, and 90–120 min. The endpoint of each chase collection period is shown along the x-axis. During each independent 30-min chase period, samples were examined under stimulated or unstimulated conditions as in Figure 6. At the conclusion of each period, the collected media and cell lysates were immunoprecipitated with anti-insulin and analyzed by SDS-PAGE and phosphorimaging. The band intensities for proinsulin, conversion intermediates, and insulin were quantitated in each sample. (A) Acquisition of stimulus competence of new secretory granules. Percentage of secretion during each time interval was calculated by the sum of proinsulin + conversion intermediates + insulin in the medium as a fraction total present in the cell lysate plus the medium collected during that time interval. The percentage of stimulus-dependent secretion, a measure of acquisition of stimulus competence, was calculated as the percentage of secretion under stimulated conditions minus the percentage of secretion under unstimulated conditions. The mean and value ranges in two identical experiments are shown (range was the same magnitude in both cell lines; shown for one set of cells only as the ranges between the cell lines overlap). (B) Processing of proinsulin to insulin within releasable secretory granules. From the stimulus-dependent secretion, the fraction comprised of proinsulin (circles), conversion intermediates (triangles), and insulin (squares) is shown as a function of time. The mean and range of values show the relative insulin production as indicated on the Figure. Note that by 2 h of chase, conversion to insulin in both sets of cells is indistinguishable.

Effects of Dominant-interfering Syn6t on Secretory Granule Biogenesis

Syn6t-10 cells that had been untreated or treated with inducer were pulse labeled with ^{35}S-amino acids for 30 min and then chased in the absence of added secretagogues for up to 4 h. Under these conditions, a modest fraction of proinsulin was secreted especially during the first 2 h of chase, and this was independent of Syn6t expression (Figure 6A). In a fifth and final hour, duplicate wells were chased further in the absence or presence of secretagogue. Regardless of Syn6t expression, the stimulus elicited release of comparable fractions of mature insulin from the regulated secretory pathway (Figure 6A). Because Syn6 has been reported to be required for homotypic fusion of small ISGs (Wendler *et al.*, 2001), it seemed possible that Syn6t might allow for the production of small ISGs that can undergo exocytosis but not fuse with each other, resulting in a smaller-than-normal granule population. We therefore performed electron microscopy at fixed magnification of INS cells not expressing or expressing the dominant-interfering Syn6t mutant for 1 d and measured the profile areas and diameters of granules under each condition. Secretory granules in ponasterone-treated INS cells have a half-life of ~17 h; therefore, the majority (65%) of granules in the 6t-10 cells were made de novo during a day of continuous Syn6t expression (Figure 6B). In the absence of Syn6t, insulin secretory granule diameters averaged 209 ± 121 nm (n = 337 granules) and in the presence of induced Syn6t expression for a full day the uncorrected diameters still averaged 209 nm ± 177 nm (n = 345 granules; the measurements were uncorrected for the variation obtained when planar sections are cut at random depths through spherical granules, which raises the standard deviations). Thus, Syn6t expression does not obviously impair the ability of insulin secretory granules to undergo regulated release or to achieve their normal final size. To look for more subtle phenotypes in initial acquisition of stimulus competence, we used a pulse-chase format to more closely examine discrete 30-min intervals during the first 2 h after proinsulin biosynthesis. Stimulus-dependent secretion of insulin-containing peptides was not less in Syn6t-expresssing cells (Figure 7A, filled symbols) compared with that in cells induced to express full-length Syn6 (open symbols). There was a delay in the endoproteolytic processing from proinsulin to insulin in Syn6t-expresing cells (Figure 7B); nevertheless, unlike the major delay in the lysosomal arrival of endocytic pathway markers (that dramatically persists after 120 min; Figures 3–5), there was no difference in the insulin content of ISGs after 120 min of chase (Figure 7B). Together, the data indicate that Syn6t expression does not cause any detectable defect in biogenesis of mature insulin secretory granules, although there is a modest lag in intragranular conversion to insulin.

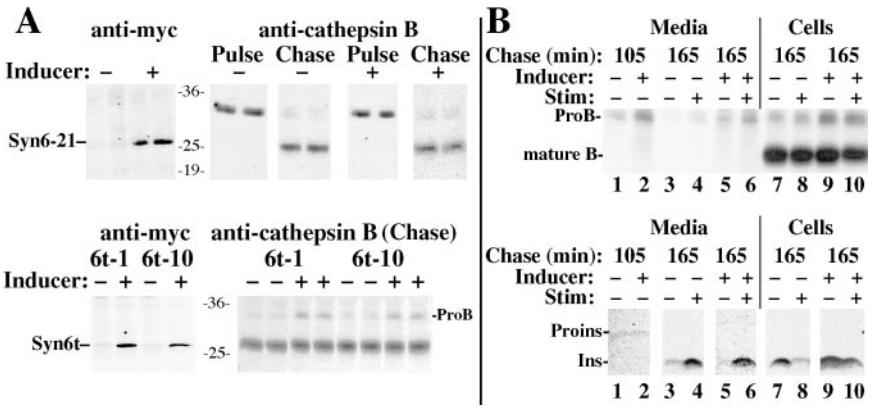

Figure 8. A minor lysosomal enzyme missorting defect is observed in INS cells upon induced expression of Syn6t. (A) Syn 6-21 cells (top) or Syn6t-1 or Syn6t-10 cells (bottom) either uninduced (−) or induced for 24 h with ponasterone (+) were pulse labeled and either lysed without chase (Pulse) or chased in the absence of secretagogues for 3 h (Chase). ProB and mature cathepsin B were recovered by immunoprecipitation with an anti-ProB antibody followed by SDS-PAGE and fluorography (right). In addition, lysates from the cells without chase were immunoprecipitated with anti-myc antibody to confirm induced expression of Syn6 or Syn6t (panels at *left*). The molecular weight markers were prestained and should be considered only approximations. (B) Syn6t-10 cells either uninduced (−) or induced for 24 h with ponasterone (+) were pulse labeled for 30 min and chased for the times indicated in the absence (−) or presence (+) of secretagogue stimulation (Stim). The identical media and cell lysate samples were immunoprecipitated with anti-ProB antibody (top) and anti-insulin antibody (bottom). The positions of ProB, mature cathepsin B (mature B), proinsulin (Proins), and insulin (Ins) are shown.

Syn6t Expression Results in Minor Missorting of Newly Synthesized Lysosomal Cathepsin B

Because Syn6t expression has obvious effects on the endocytic pathway (Figures 3–5), we proceeded to study indirectly the effect of Syn6t expression on the recycling/availability of mannose phosphate receptors by examining newly synthesized lysosomal enzyme delivery to lysosomes in these cells (as measured by intracellular conversion of procathepsin B [ProB] to the mature lysosomal form). In the absence or presence of expression of the full-length Syn6 (Figure 8A, top left), the ProB precursor is initially present at the end of the pulse labeling but is largely converted to mature B after a 4-h chase (Figure 8A, top right). Identical results were obtained in control INS and INS39 cells (our unpublished data). On induced expression of Syn6t (in either the 6t-1 or 6t-10 clones; Figure 8A, bottom left), ProB delivery to lysosomes at 4-h chase was incomplete in comparison with the cells in the absence of inducer (Figure 8A, bottom right). However, the magnitude of this effect was clearly small because the recovery of newly synthesized mature cathepsin B from the induced cells was not appreciably diminished from that in uninduced cells (Figure 8A, bottom right). Overall from three experiments, there was an increase of 10 ± 5% of intracellular ProB at the end of the chase as a result of the expression of Syn6t.

Previously published studies of INS cells have indicated that most newly synthesized ProB sorting has occurred within 1.75 h of chase, during which there is modest constitutive and constitutive-like secretion; thereafter, there is little or no unstimulated or stimulated release of ProB (Kuliawat *et al*., 1997; Turner and Arvan, 2000). To determine the extent of spillover of ProB from the TGN into ISGs of Syn6t-expressing cells, we examined unstimulated and stimulated secretion for 1 h beginning after the first 1.75 h had elapsed. During the first 1.75 h in either the absence or presence of inducer, there was very little newly synthesized proinsulin released (Figure 8B, bottom). Furthermore, in agreement with earlier results (Figure 6A), there was clear stimulus-dependent release of processed insulin recovered during the ensuing hour (Figure 8B, bottom). From the identical samples, cells with Syn6t expression exhibited an increase in the unstimulated release of ProB during the first 1.75 h, consistent with modest missorting into constitutive and constitutive-like secretory pathways (Figure 8B, top, lane 2). Moreover, during the ensuing hour in cells treated with inducer, the stimulus-dependent release of ProB (Figure 8B, top, compare lanes 5 and 6) was of a small magnitude such that it resulted in little depletion of the labeled cathepsin B remaining in the cell lysate (lanes 9 and 10), despite stimulus-dependent insulin release from the same samples sufficient to cause marked insulin depletion from the cells (lanes 9 and 10, bottom). These data confirm that the overall extent of ProB missorting into constitutive and constitutive-like pathways (as well as ProB persistence in secretory granules) was relatively minor, and most intracellular ProB that did persist at 165 min of chase was not depleted by secretagogue and was therefore likely to already be in transit beyond the secretory pathway, i.e., delayed while en route through the endosomal system.

Recycling to the TGN in Syn6t-expressing INS Cells

Recycling of TGN resident proteins can be followed by antibody- or other tagging of the subpopulation of molecules that are cycling via the plasmalemma and then following the surface-tagged molecules as they return to the TGN via the endosomal system (Gartung *et al*., 1985; Molloy *et al*., 1994; Banting and Ponnambalam, 1997; Varlamov and Fricker, 1998). In numerous preliminary experiments, we examined endocytic return of surface-tagged endogenous carboxypeptidase D and found that, slower than previously reported for recycling of this antigen in AtT-20 cells (Varlamov and Fricker, 1998), a 2-h period of continuous antibody uptake was optimal to achieve a concentrated TGN-based signal of surface-tagged molecules in the entire population of INS cells. With this in mind, we then performed a series of experiments in INS cells expressing or not expressing Syn6t.

Figure 9 experiment ① shows the transient expression of a chimeric protein in which the N-terminal lumenal domain of serum albumin was attached to the transmembrane and cytosolic domains of CPD (Alb-CPD). In cells not expressing Syn6t, (top row of panels), a 2-h antibody uptake delivered Alb-CPD in transfected cells (red) to the compartment positive for endogenous TGN38 (green). In three independent experiments, this was the case in 100% of the cells. By contrast, in three different images of INS cells with induced expression of Syn6t, different degrees of delayed delivery of Alb-CPD could be seen (experiment ①, bottom row of panels; some of the cells marked with small arrows). Quantitatively, 96% of Syn6t-expressing cells failed to show Alb-CPD

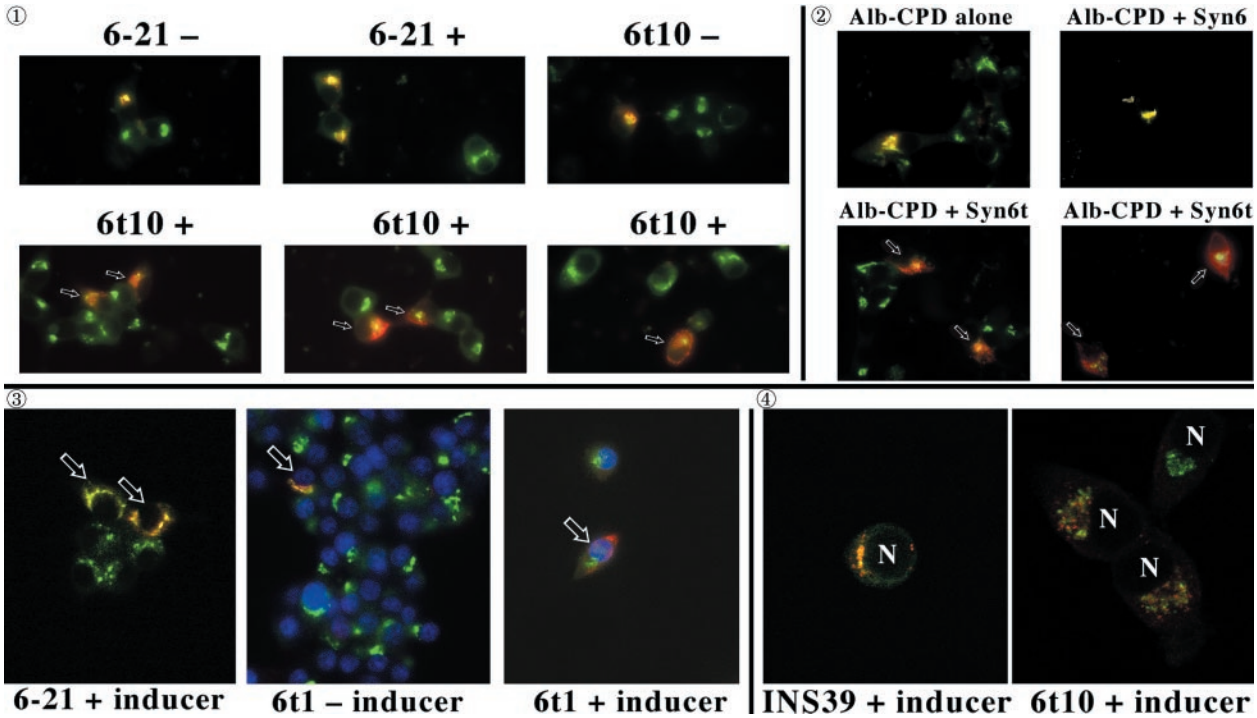

Figure 9. Transient expression and recycling of albumin-CPD and Tac-TGN38 chimeras in INS cells. Experiment ①: Syn 6-21 cells or Syn6t-10 cells were transfected with a plasmid encoding Alb-CPD and either uninduced (−) or induced for 24 h with ponasterone (+) before a 2-h continuous uptake with an anti-albumin polyclonal antibody (in red) as well as the immunofluorescent distribution of TGN38 by using a mAb (in green). In cells expressing Syn6t, transfected cells are marked with small arrows. Experiment ②: INS cells were transfected with Alb-CPD, full-length Syn6, or Syn6t-encoding plasmids, alone or in combination as indicated (double transfections used a 5:1 ratio of syntaxin DNA to Alb-CPD DNA). The cells were then labeled as in experiment ①. In cells expressing Syn6t, transfected cells are marked with small arrows. Experiment ③: Syn 6-21 cells or Syn6t-1 cells were transfected with a plasmid encoding Tac-TGN38 and either uninduced (−) or induced for 24 h with ponasterone (+) before a 2-h continuous uptake with a mAb anti-Tac (in red) as well as the immunofluorescent distribution by using a polyclonal anti-TGN38 lumenal domain (in green). In the latter two panels, the nuclei are also stained with 4,6-diamidino-2-phenylindole (in blue). Transfected cells are marked with arrows. Experiment ④: INS39 cells or Syn6t-10 cells were transfected, induced with ponasterone, and labeled as in experiment ②, except that the cells were examined by confocal fluorescence microscopy.

colocalization with TGN38. In experiment ②, to eliminate the addition of inducer as a potential variable, INS cells were transiently transfected either with plasmid encoding Alb-CPD alone, Alb-CPD plus full-length Syn6, or Alb-CPD plus Syn6t (an unequal ratio of the two plasmids in double transfection was used to ensure that all cells transfected with Alb-CPD also received a Syn6-containing construct). Once again, in cells not expressing Syn6t (top), Alb-CPD reached the TGN (in 100% of cells) whereas in cells expressing Syn6t, Alb-CPD arrival in the TGN was delayed (bottom) in all transfected cells. This phenotype was not related to overexpression of Alb-CPD per se because mislocalization of Alb-CPD was exclusive to cells expressing Syn6t. Moreover, an identical phenotype was observed for continuous 2-h uptake of anti-CPD (to follow the endogenous membrane protein) in cells transiently transfected to express full-length Syn6 (100% of transfected cells achieving a tight juxtanuclear localization of CPD) or Syn6t (only 12% of cells achieving this localization).

These experiments were extended to use transiently expressed Tac-TGN38 (Mallard *et al.*, 2002). In Figure 9, experiment ③, cells not expressing Syn6t delivered the expressed Tac-TGN38 (red, cells marked with arrows) to the TGN38-positive compartment (green) and cells expressing Syn6t showed delayed delivery of Tac-TGN38 (right). Finally, by using confocal immunofluorescent microscopy in experiment ④, it was apparent that whereas INS cells not expressing Syn6t showed excellent Tac-TGN38 delivery to the TGN38-positive compartment, even in Syn6t-expressing cells where Tac-TGN38 reached a predominant juxtanuclear location (nuclear position denoted with "N"), the chimera still did not colocalize with the TGN marker in these cells. Quantitatively, when combining all experiments expressing either Alb-CPD or Tac-TGN38, of INS cells not expressing Syn6t, 100% achieved colocalization of these markers with endogenous TGN38, whereas for cells that do express Syn6t, 5.6% of cells achieved colocalization with TGN38, 13.9% achieved partial colocalization, and 80.5% of cells achieved no colocalization. These data are consistent with results in Chinese hamster ovary cells in which efficient endosomal Tac-TGN38 return to the TGN is kinetically impaired by overexpressing a construct very similar to Syn6t (Mallard *et al.*, 2002).

Syn6t Expression Alters Vti1b Distribution in Pancreatic β-Cells

At the molecular level, the role of Syn6 in efficient endosomal delivery of proteins might be explained by associations with a number of potential Syn6-interacting proteins (Simonsen *et al.*, 1999; Nagamatsu *et al.*, 2001; Wendler and Tooze, 2001). Using available antibodies, we could not convincingly demonstrate coimmunoprecipitation of Syn7,

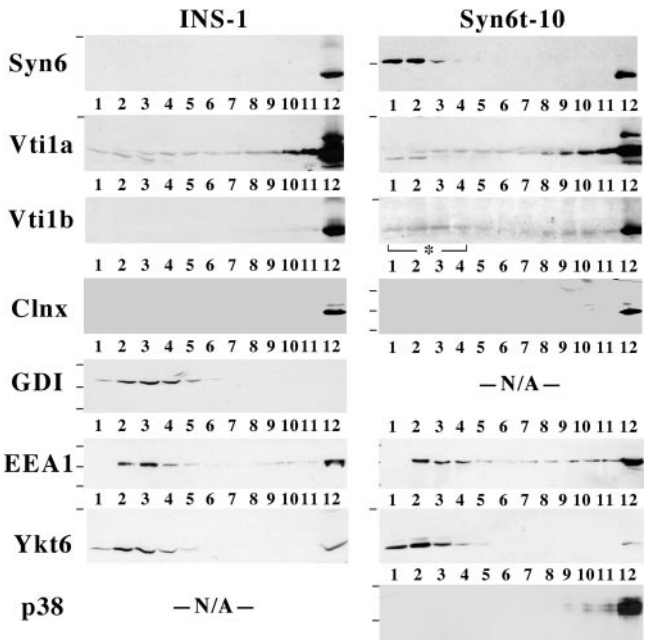

Figure 10. Syn6t expression alters the distribution of Vti1b in INS cells. Control INS cells or Syn6t-10 cells were treated with ponasterone for 24 h, lysed, and the cell extracts loaded on sucrose velocity gradients. The numbered fractions run from top to bottom of the sucrose gradients. Each fraction was analyzed by SDS-PAGE and immunoblotting with the antibodies indicated. Small horizontal lines to the left of the gels indicate positions of prestained molecular mass markers that allowed for identification of the correct region. Clnx, calnexin; EEA1, early endosomal antigen 1; p38, synaptophysin.

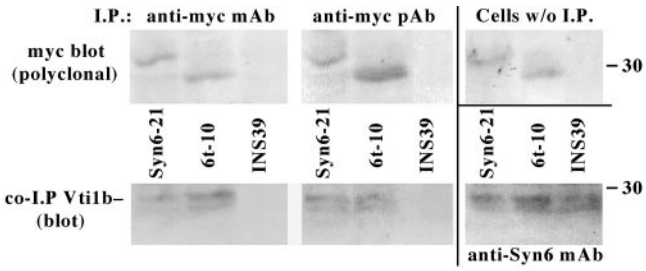

Figure 11. Vti1b association with Syn6t and Syn6 in INS cells. The cell lines indicated were immunoprecipitated with anti-myc mAb or anti-myc polyclonal antibody, which were then subjected to SDS-PAGE and immunoblotting. All three lower panels show immunoblotting with anti-Vti1b; note that from control INS39 cells no Vti1b can be coprecipitated with anti-myc (left and middle) although Vti1b can be coprecipitated when the cells are immunoprecipitated with anti-Syn6 (bottom right). The upper panels all show myc Western blotting with polyclonal anti-myc to confirm direct immunoprecipitation of the myc-tagged Syn6 full-length and Syn6t constructs as well as the presence of these bands in the original cell lysates (top right).

Vti1a, Ykt6, mVps45, or EEA1 with Syn6t in INS cells. We therefore tried another approach: because Syn6t has different sedimentation properties to that of full-length Syn6 (Figure 2), INS cells expressing or not expressing Syn6t were lysed in the complete absence of detergents and postnuclear supernatants were analyzed by 5–20% sucrose-velocity gradient centrifugation to examine the relative distribution of potential interactors. As shown in Figure 10, Western blotting for Syn6 in INS-1 cells (left set of panels) showed the endogenous protein recovered exclusively at the bottom of the gradient (fraction 12). This also matched the distribution of endogenous Vti1b (Figure 10), and the integral membrane protein marker calnexin (Figure 10, Clnx) was similarly distributed. In 6t-10 cells (right set of panels), endogenous Syn6 showed the same distribution while induced expression of Syn6t was recovered in the upper four fractions (top gradient, upon overexposure, a very small fraction of Syn6t was also recovered in fraction 12), and this distribution of soluble Syn6t is similar to that observed for the soluble GDI marker protein in control cells. Two SNARE proteins were recovered both in apparently soluble forms as well as at the bottom of the gradient (in markedly different proportions), namely, Vti1a and Ykt6; the latter distribution has also been reported by others (Hasegawa *et al.*, 2003). However, neither of these two proteins, nor the early endosomal antigen EEA1, was unequivocally altered by Syn6t expression. By contrast, upon expression of Syn6t, the distribution of Vti1b was distinctly shifted in part to the uppermost four fractions of the sucrose-velocity gradient (right set of panels). We do not know whether the redistribution of a subset of Vti1b molecules reflects their extraction from membranes because the membrane anchor of Vti1b contains the highly unusual negatively charged (Glu) residue midway along its transmembrane domain (Advani *et al.*, 1998). We also entertained the possibility that this shift could reflect Vti1b relocation into a population of microvesicles (Antonin *et al.*, 2000) rather than to a soluble cytosolic population, but this seemed unlikely because synaptic-like microvesicles are still recovered at the bottom of the detergent-free gradient, as judged by the distribution of the marker synaptophysin/p38 (Figure 10, bottom).

Vti1 in yeast is required for all traffic to the yeast lysosome (von Mollard *et al.*, 1997) and human Vti1 can functionally substitute for yeast Vti1 in *vti1* mutant yeast (von Mollard and Stevens, 1998). The mammalian Vti1b in particular is localized to endosomes (Kreykenbohm *et al.*, 2002), and Syn6 is known to form a complex with Vti1b in other cell types (Xu *et al.*, 1998; Wade *et al.*, 2001). We therefore used an immunoprecipitation-Western coprecipitation assay to determine whether Vti1b could associate with Syn6 and Syn6t in INS cells. Syn6-21, 6t-10, or control INS39 cells were immunoprecipitated with anti-myc mAb or anti-myc polyclonal antibody. These immunoprecipitates were immunoblotted with polyclonal anti-myc to confirm immunoprecipitation (Figure 11, top left and top middle). As expected, no blottable myc band could be recovered from control INS39 cells. Myc-tagged protein expression was also confirmed by direct immunoblotting of lysates of cells that had not been previously immunoprecipitated (Figure 11, top right). Anti-myc immunoprecipitates subjected to SDS-PAGE and electrotransfer were immunoblotted with anti-Vti1b antibody (bottom left and bottom middle). No Vti1b could be immunoblotted from immunoprecipitates of cells not expressing a myc-tagged Syn6 protein. However, Vti1b was coprecipitated using anti-myc in lysates of cells with induced expression of either full-length Syn6 or Syn6t. Finally, all three of the cell lines could generate coprecipitation of Vti1b when the initial immunoprecipitation was performed with anti-Syn6 mAb (Figure 11, bottom right). Together, the data in Figures 10 and 11 are consistent with Syn6t competing for a subset of potential Syn6 SNARE interactions, including Vti1b within the endosomal system.

DISCUSSION

Dominant Negative Effects of Syn6t on the Endocytic Pathway

Syn6 is a long-lived protein (Figure 1B) that is localized to endosomes and the TGN/ISGs (Bock *et al.*, 1996, 1997; Klumperman *et al.*, 1998; Simonsen *et al.*, 1999; Steegmaier *et al.*, 1999; Watson and Pessin, 2000; Wade *et al.*, 2001; Wendler *et al.*, 2001). Thus, it is widely believed that Syn6 regularly recycles and, kinetically speaking, exit from endosomal intermediates and the biosynthetic pathway represents the slowest steps in the Syn6 cycling itinerary. The issue addressed in the present study is where does the Syn6 SNARE potentially participate in a rate-limiting step in protein trafficking, rather than functioning primarily as a cargo protein. Based on actions of the dominant-negative Syn6t in INS cells, the evidence presented implicates a primary activity of Syn6 in the endosomal system of pancreatic β-cells.

The predominant distribution of Syn6 in endosomes and the TGN in itself might suggest that Syn6 participates directly in endosome–TGN return; indeed, a construct called $Syn6_{cyto}$ (which is nearly identical to our Syn6t) has been reported to inhibit TGN return of a Tac-TGN38 chimera (Mallard *et al.*, 2002), and we have confirmed these findings upon Syn6t expression in INS cells both for Tac-TGN38 and for Alb-CPD (Figure 9). This inhibition represents primarily a kinetic slowing of the return route, whereas the TGN exit step remains slow or slower, because the steady-state distributions of TGN markers (CPD and TGN38) do not seem altered (Figures 1C and 8). Similarly, upon Syn6t expression in INS cells, there is a significant kinetic defect in endocytic cargo delivery from the cell surface to lysosomes as measured biochemically (Figure 3A) or morphologically (Figures 4 and 5A). This defect seems to occur downstream of the branchpoint for transferrin recycling (Figure 3B) yet upstream of mannose-phosphate receptor-enriched late endosomes (Figure 5B). On expression in INS cells (Figures 1 and 2), we observe coimmunoprecipitation of Syn6t with Vti1b (Figure 11) (an endosomal SNARE; Kreykenbohm *et al.*, 2002) and a change in the intracellular distribution of Vti1b (Figure 10), consistent with the idea that Syn6t works by competing for endosomal Syn6 SNARE partners (Simonsen *et al.*, 1999; Mills *et al.*, 2001; Wade *et al.*, 2001; Kreykenbohm *et al.*, 2002; Mallard *et al.*, 2002), altering the intracellular distribution of at least one, to influence cargo progression from early endosomes to lysosomes or the TGN.

Effects of Syn6t Expression on the Biosynthetic Pathway

In the literature, one potential Syn6-interactor (endobrevin/VAMP8) has been implicated in playing a physiological role in the exo-endocytosis cycle of insulin secretory granule (Nagamatsu *et al.*, 2001). Even more important to the current considerations is the longstanding view that new secretory granule biogenesis involves reutilizing many secretory granule membrane constituents that have recycled via the endocytic pathway (Farquhar, 1983). Given the clear positive findings of the current study implicating Syn6 function within the endosomal system, one of our central goals was then to test whether Syn6t could interfere significantly with secretory granule formation. Indeed, a recent report has suggested that Syn6 is involved in secretory granule biogenesis by facilitating homotypic fusion of ISGs, based on an in vitro fusion assay using ISGs from PC12 cells (Wendler *et al.*, 2001). However, positive evidence indicating homotypic fusion of ISGs in live regulated secretory cells, even PC12 cells, has not yet been obtained (Rudolf *et al.*, 2001), nor has this step yet been shown to be essential for granule biogenesis in endocrine, exocrine, or neural cells. Moreover, a purified recombinant soluble Syn6 construct containing $Syn6_{2–231}$ (only slightly smaller than our $Syn6t_{1–236}$) does not inhibit readout in the in vitro assay (Wendler *et al.*, 2001). In agreement, the present data indicate that Syn6t does not obviously impair the cross-sectional area of the mature insulin granule population (Figure 6) or the formation of new secretory granules as judged by acquisition of secretagogue-stimulated exocytosis (Figure 7A), even though it does produce overt effects on the endosomal system.

What is observed in the biosynthetic pathway upon Syn6t expression is a modest lag in intragranular conversion to insulin (Figure 7B) and a small lysosomal enzyme missorting phenotype (Figure 8), including increases in the amount of ProB spilling into constitutive and constitutive-like secretory pathways and exhibiting abnormally prolonged residence in secretory granules as well as in postsecretory (i.e., endosomal) compartments. However, because mannose-phosphate receptor-dependent trafficking of ProB is only marginally affected, we suggest that the endosomal step(s) inhibited by Syn6t expression is likely to be largely proximal to the endosomal site of entry of most mannose-phosphate receptors. This is also consistent with kinetic slowing of SFV endocytic transport at a site proximal to the steady-state distribution of mannose-phosphate receptors (Figure 5B). Moreover, the fact that the steady-state distribution of TGN proteins is not obviously affected upon Syn6t expression provides a further indication that secretory pathway operations are likely to proceed relatively normally in spite of slowed kinetics of protein return from the endosomal system.

Thus, we conclude that Syn6t provides only modest and potentially indirect interference with regulated and constitutive secretory pathways, and in TGN sorting of lysosomal enzymes.

In summary, the data obtained in the pancreatic β-cell line INS-1 suggest that Syn6 plays a potentially rate-limiting role in endocytic delivery both to lysosomes and the TGN. Given the recent finding that certain insulin secretory granule membrane proteins may be irreversibly cleaved upon stimulated exocytosis at the plasma membrane (Ort *et al.*, 2001), and thus cannot be reused intact, we believe the question of how important endosome-to-TGN return really is for ongoing secretory granule biogenesis remains open, and needs to be revisited.

ACKNOWLEDGMENTS

This work was primarily supported by National Institutes of Health DK-48280 (to P.A.), DK-56027 (to R.K.), DK-55711 (to L.D.F.), and DK-57689 (to T.E.M). We are indebted to Kathy Anderson (a rotation student in the Arvan laboratory) for initiating transfections that produced ecdysone receptor-expressing INS cells. We thank Dr. R.G. Pestell (Georgetown University) for advice in setting up the ecdysone-inducible system and for providing an aliquot of mouse mAb against the ecdysone receptor. We are grateful to Dr. M. Kielian (Albert Einstein College of Medicine) who assisted with the radiolabeled Semliki Forest Virus endocytosis assays. We thank Drs. S. Milgram (University of North Carolina) and D. Shields (Albert Einstein College of Medicine) for gifts of antibodies. We acknowledge Carolyn Marks and Frank Macaluso (Einstein Analytical Imaging Facility) for technical assistance. We thank members of the Arvan laboratory for helpful discussions.

REFERENCES

Advani, R.J., Bae, H.R., Bock, J.B., Chao, D.S., Doung, Y.C., Prekeris, R., Yoo, J.S., and Scheller, R.H. (1998). Seven novel mammalian SNARE proteins localize to distinct membrane compartments. J. Biol. Chem. *273*, 10317–10324.

Antonin, W., Riedel, D., and von Mollard, G.F. (2000). The SNARE Vti1a-beta is localized to small synaptic vesicles and participates in a novel SNARE complex. J. Neurosci. *20*, 5724–5732.

Banting, G., and Ponnambalam, S. (1997). TGN38 and its orthologues: roles in post-TGN vesicle formation and maintenance of TGN morphology. Biochim. Biophys. Acta Mol. Cell Res. *1355*, 209–217.

Bock, J.B., Klumperman, J., Davanger, S., and Scheller, R.H. (1997). Syntaxin 6 functions in trans-Golgi network vesicle trafficking. Mol. Biol. Cell *8*, 1261–1271.

Bock, J.B., Lin, R.C., and Scheller, R.H. (1996). A new syntaxin family member implicated in targeting of intracellular transport vesicles. J. Biol. Chem. *271*, 17961–17965.

Bock, J.B., Matern, H.T., Peden, A.A., and Scheller, R.H. (2001). A genomic perspective on membrane compartment organization. Nature *409*, 839–841.

Collins, R.F., Schreiber, A.D., Grinstein, S., and Trimble, W.S. (2002). Syntaxins 13 and 7 function at distinct steps during phagocytosis. J. Immunol. *169*, 3250–3256.

Dascher, C., and Balch, W. (1996). Mammalian Sly1 regulates syntaxin 5 function in endoplasmic reticulum to Golgi transport. J. Biol. Chem. *271*, 15866–15869.

Dittié, A.S., Thomas, L., Thomas, G., and Tooze, S.A. (1997). Interaction of furin in immature secretory granules from neuroendocrine cells with the AP-1 adaptor complex is modulated by casein kinase II phosphorylation. EMBO J. *16*, 4859–4870.

Eaton, B.A., Haugwitz, M., Lau, D., and Moore, H.P. (2000). Biogenesis of regulated exocytotic carriers in neuroendocrine cells. J. Neurosci. *20*, 7334–7344.

Farquhar, M.G. (1983). Multiple pathways of exocytosis, endocytosis, and membrane recycling: validation of a Golgi route. Fed. Proc. *42*, 2407–2413.

Feng, L., and Arvan, P. (2003). The trafficking of alpha1-antitrypsin, a post-Golgi secretory pathway marker, in INS-1 pancreatic beta cells. J. Biol. Chem. *278*, 31486–31494.

Fukuda, R., McNew, J.A., Weber, T., Parlati, F., Engel, T., Nickel, W., Rothman, J.E., and Sollner, T.H. (2000). Functional architecture of an intracellular membrane t-SNARE. Nature *407*, 198–202.

Gartung, C., Braulke, T., Hasilik, A., and von Figura, K. (1985). Internalization of blocking antibodies against mannose-6-phosphate specific receptors. EMBO J. *4*, 1725–1730.

Geelen, D., Leyman, B., Batoko, H., Di Sansebastiano, G.P., Moore, I., Blatt, M.R., and Di Sansabastiano, G.P. (2002). The abscisic acid-related SNARE homolog NtSyr1 contributes to secretion and growth: evidence from competition with its cytosolic domain. Plant Cell *14*, 387–406.

Ghosh, R.N., Mallet, W.G., Soe, T.T., McGraw, T.E., and Maxfield, F.R. (1998). An endocytosed TGN38 chimeric protein is delivered to the TGN after trafficking through the endocytic recycling compartment in CHO cells. J. Cell Biol. *142*, 923–936.

Griffiths, G., Hoflack, B., Simons, K., Mellman, I., and Kornfeld, S. (1988). The mannose 6-phosphate receptor and the biogenesis of lysosomes. Cell *52*, 329–341.

Hasegawa, H., Zinsser, S., Rhee, Y., Vik-Mo, E.O., Davanger, S., and Hay, J.C. (2003). Mammalian ykt6 is a neuronal SNARE targeted to a specialized compartment by its profilin-like amino terminal domain. Mol. Biol. Cell *14*, 698–720.

Hinners, I., Wendler, F., Fei, H., Thomas, L., Thomas, G., and Tooze, S.A. (2003). AP-1 recruitment to VAMP4 is modulated by phosphorylation-dependent binding of PACS-1. EMBO Rep. *4*, 1–8.

Hu, C., Ahmed, M., Melia, T.J., Sollner, T.H., Mayer, T., and Rothman, J.E. (2003). Fusion of cells by flipped SNAREs. Science *300*, 1745–1749.

Hua, Y., and Scheller, R.H. (2001). Three SNARE complexes cooperate to mediate membrane fusion. Proc. Natl. Acad. Sci. USA *98*, 8065–8070.

Humphrey, J.S., Peters, P.J., Yuan, L.C., and Bonifacino, J.S. (1993). Localization of TGN38 to the trans-Golgi network: involvement of a cytoplasmic tyrosine-containing sequence. J. Cell Biol. *120*, 1123–1135.

Kalinina, E.V., and Fricker, L.D. (2003). Palmitoylation of carboxypeptidase D. Implications for intracellular trafficking. J. Biol. Chem. *278*, 9244–9249.

Kasai, K., and Akagawa, K. (2001). Roles of the cytoplasmic and transmembrane domains of syntaxins in intracellular localization and trafficking. J. Cell Sci. *114*, 3115–3124.

Kielian, M., Jungerwirth, S., Sayad, K.U., and DeCandido, S. (1990). Biosynthesis, maturation, and acid activation of the Semliki Forest virus fusion protein. J. Virol. *64*, 4614–4624.

Klumperman, J., Kuliawat, R., Griffith, J.M., Geuze, H.J., and Arvan, P. (1998). Mannose 6-phosphate receptors are sorted from immature secretory granules via AP-1, clathrin, and syntaxin 6-positive vesicles. J. Cell Biol. *141*, 359–371.

Kreykenbohm, V., Wenzel, D., Antonin, W., Atlachkine, V., and von Mollard, G.F. (2002). The SNAREs vti1a and vti1b have distinct localization and SNARE complex partners. Eur. J. Cell Biol. *81*, 273–280.

Kuliawat, R., and Arvan, P. (1992). Protein targeting via the "constitutive-like" secretory pathway in isolated pancreatic islets: passive sorting in the immature granule compartment. J. Cell Biol. *118*, 521–529.

Kuliawat, R., and Arvan, P. (1994). Distinct molecular mechanisms for protein sorting within immature secretory granules of pancreatic β-cells. J. Cell Biol. *126*, 77–86.

Kuliawat, R., Klumperman, J., Ludwig, T., and Arvan, P. (1997). Differential sorting of lysosomal enzymes out of the regulated secretory pathway in pancreatic β-cells. J. Cell Biol. *137*, 595–608.

Li, G., Alexander, E.A., and Schwartz, J.H. (2003). Syntaxin isoform specificity in the regulation of renal H+-ATPase exocytosis. J. Biol. Chem. *278*, 19791–19797.

Low, S.H., Li, X., Miura, M., Kudo, N., Quinones, B., and Weimbs, T. (2003). Syntaxin 2 and endobrevin are required for the terminal step of cytokinesis in mammalian cells. Dev. Cell. *4*, 753–759.

Luzio, J.P., Brake, B., Banting, G., Howell, K.E., Braghetta, P., and Stanley, K.K. (1990). Identification, sequencing and expression of an integral membrane proteins of the trans-Golgi network (TGN38). Biochem. J. *270*, 97–102.

Mallard, F., Tang, B.L., Galli, T., Tenza, D., Saint-Pol, A., Yue, X., Antony, C., Hong, W., Goud, B., and Johannes, L. (2002). Early/recycling endosomes-to-TGN transport involves two SNARE complexes and a Rab6 isoform. J. Cell Biol. *156*, 653–664.

Marks, M.S., Woodruff, L., Ohno, H., and Bonifacino, J.S. (1996). Protein targeting by tyrosine- and di-leucine-based signals: evidence for distinct saturable components. J. Cell Biol. *135*, 341–354.

Martys, J.L., Wjasow, C., Gangi, D.M., Kielian, M.C., McGraw, T.E., and Backer, J.M. (1996). Wortmannin-sensitive trafficking pathways in Chinese hamster ovary cells. Differential effects on endocytosis and lysosomal sorting. J. Biol. Chem. *271*, 10953–10962.

Milgram, S.L., Eipper, B.A., and Mains, R.E. (1994). Differential trafficking of soluble and integral membrane secretory granule-associated proteins. J. Cell Biol. *124*, 33–41.

Mills, I.G., Urbe, S., and Clague, M.J. (2001). Relationships between EEA1 binding partners and their role in endosome fusion. J. Cell Sci. *114*, 1959–1965.

Misura, K.M., Bock, J.B., Gonzalez, L.C.J., Scheller, R.H., and Weis, W.I. (2002). Three-dimensional structure of the amino-terminal domain of syntaxin 6, a SNAP-25 C homolog. Proc. Natl. Acad. Sci. USA *99*, 9184–9189.

Molinete, M., Dupuis, S., Brodsky, F.M., and Halban, P.A. (2001). Role of clathrin in the regulated secretory pathway of pancreatic beta-cells. J. Cell Sci. *114*, 3059–3066.

Molloy, S.S., Anderson, E.D., Jean, F., and Thomas, G. (1999). Bi-cycling the furin pathway: from TGN localization to pathogen activation and embryogenesis. Trends Cell Biol. 28–35.

Molloy, S.S., Thomas, L., VanSlyke, J.K., Stenberg, P.E., and Thomas, G. (1994). Intracellular trafficking and activation of the furin proprotein convertase: localization to the TGN and recycling from the cell surface. EMBO J. *13*, 18–33.

Nagamatsu, S., Nakamichi, Y., Watanabe, T., Matsushima, S., Yamaguchi, S., Ni, J., Itagaki, E., and Ishida, H. (2001). Localization of cellubrevin-related peptide, endobrevin, in the early endosome in pancreatic beta cells and its physiological function in exo-endocytosis of secretory granules. J. Cell Sci. *114*, 219–227.

Neerman-Arbez, M., and Halban, P.A. (1993). Novel, non-crinophagic, degradation of connecting peptide (C-peptide) in transformed pancreatic beta cells. J. Biol. Chem. *268*, 16248–16252.

Olson, A.L., Knight, J.B., and Pessin, J.E. (1997). Syntaxin 4, VAMP2, and/or VAMP3/cellubrevin are functional target membrane and vesicle SNAP receptors for insulin-stimulated GLUT4 translocation in adipocytes. Mol. Cell. Biol. *17*, 2425–2435.

Orci, L., Halban, P., Amherdt, M., Ravazzola, M., Vassalli, J.D., and Perrelet, A. (1984). Nonconverted, amino acid analog-modified proinsulin stays in a Golgi-derived clathrin-coated membrane compartment. J. Cell Biol. *99*, 2187–2192.

Ort, T., Voronov, S., Guo, J., Zawalich, K., Froehner, S.C., Zawalich, W., and Solimena, M. (2001). Dephosphorylation of beta2-syntrophin and Ca2+/mu-calpain-mediated cleavage of ICA512 upon stimulation of insulin secretion. EMBO J. *20*, 4013–4023.

Parlati, F., McNew, J.A., Fukuda, R., Miller, R., Sollner, T.H., and Rothman, J.E. (2000). Topological restriction of SNARE-dependent membrane fusion. Nature *407*, 194–198.

Parlati, F., Varlamov, O., Paz, K., McNew, J.A., Hurtado, D., Sollner, T.H., and Rothman, J.E. (2002). Distinct SNARE complexes mediating membrane fusion in Golgi transport based on combinatorial specificity. Proc. Natl. Acad. Sci. USA *99*, 5424–5429.

Regazzi, R., Sadoul, K., Meda, P., Kelly, R.B., Halban, P.A., and Wollheim, C.B. (1996). Mutational analysis of VAMP domains implicated in Ca2+-induced insulin exocytosis. EMBO J. *15*, 6951–6959.

Rudolf, R., Salm, T., Rustom, A., and Gerdes, H.H. (2001). Dynamics of immature secretory granules: role of cytoskeletal elements during transport, cortical restriction, and F-actin-dependent tethering. Mol. Biol. Cell *12*, 1353–1365.

Scales, S.J., Chen, Y.A., Yoo, B.Y., Patel, S.M., Doung, Y.C., and Scheller, R.H. (2000). SNAREs contribute to the specificity of membrane fusion. Neuron *26*, 457–464.

Simonsen, A., Gaullier, J.M., D'Arrigo, A., and Stenmark, H. (1999). The rab5 effector EEA1 interacts directly with syntaxin-6. J. Biol. Chem. *274*, 28857–28860.

Steegmaier, M., Klumperman, J., Foletti, D.L., Yoo, J.S., and Scheller, R.H. (1999). Vesicle-associated membrane protein 4 is implicated in trans-Golgi network vesicle trafficking. Mol. Biol. Cell *10*, 1957–1972.

Tooze, S.A., Flatmark, T., Tooze, J., and Huttner, W.B. (1991). Characterization of the immature secretory granule, an intermediate in granule biogenesis. J. Cell Biol. *115*, 1491–1504.

Turner, M., and Arvan, P. (2000). Protein traffic from the secretory pathway to the endosomal system in pancreatic β-cells. J. Biol. Chem. *275*, 14025–14030.

Urbe, S., Page, L.J., and Tooze, S.A. (1998). Homotypic fusion of immature secretory granules during maturation in a cell-free assay. J. Cell Biol. *143*, 1831–1844.

Varlamov, O., and Fricker, L.D. (1998). Intracellular trafficking of metallocarboxypeptidase D in AtT-20 cells: localization to the trans-Golgi network and recycling from the cell surface. J. Cell Sci. *111*, 877–885.

von Mollard, G.F., Nothwehr, S.F., and Stevens, T.H. (1997). The yeast v-SNARE Vti1p mediates two vesicle transport pathways through interactions with the t-SNAREs Sed5p and Pep12p. J. Cell Biol. *137*, 1511–1524.

von Mollard, G.F., and Stevens, T.H. (1998). A human homolog can functionally replace the yeast vesicle-associated SNARE Vti1p in two vesicle transport pathways. J. Biol. Chem. *273*, 2624–2630.

Wade, N., Bryant, N.J., Connolly, L.M., Simpson, R.J., Luzio, J.P., Piper, R.C., and James, D.E. (2001). Syntaxin 7 complexes with mouse Vps10p tail interactor 1b, syntaxin 6, vesicle-associated membrane protein (VAMP)8, and VAMP7 in b16 melanoma cells. J. Biol. Chem. *276*, 19820–19827.

Watson, R.T., and Pessin, J.E. (2000). Functional cooperation of two independent targeting domains in syntaxin 6 is required for its efficient localization in the trans-Golgi network of 3T3L1 adipocytes. J. Biol. Chem. *275*, 1261–1268.

Wendler, F., Page, L., Urbe, S., and Tooze, S.A. (2001). Homotypic fusion of immature secretory granules during maturation requires syntaxin 6. Mol. Biol. Cell *12*, 1699–1709.

Wendler, F., and Tooze, S. (2001). Syntaxin *6*, the promiscuous behaviour of a SNARE protein. Traffic *2*, 606–611.

Wheeler, M.B., Sheu, L., Ghai, M., Bouquillon, A., Grondin, G., Weller, U., Beaudoin, A.R., Bennett, M.K., Trimble, W.S., and Gaisano, H. (1996). Characterization of SNARE protein expression in beta cell lines and pancreatic islets. Endocrinology *137*, 1340–1348.

Xu, H., Boulianne, G.L., and Trimble, W.S. (2002). Drosophila syntaxin 16 is a Q-SNARE implicated in Golgi dynamics. J. Cell Sci. *115*, 4447–4455.

Xu, Y., Wong, S.H., Tang, B.L., Subramaniam, V.N., Zhang, T., and Hong, W. (1998). A 29-kilodalton Golgi SNARE (Vti1-rp2) Implicated in protein trafficking in the secretory pathway. J. Biol. Chem. *273*, 21783–21789.